n-Alkanes and polycyclic aromatic hydrocarbons in total suspended particulates from the southeastern Tibetan Plateau: Concentrations, seasonal variations, and sources

Yang Chen [a], Junji Cao [a,b,*], Jing Zhao [b], Hongmei Xu [a], Richard Arimoto [a], Gehui Wang [a], Yongming Han [a], Zhenxing Shen [b], Guohui Li [a]

[a] Key Lab of Aerosol Science & Technology, SKLLQG, Institute of Earth Environment, Chinese Academy of Science, Xi'an, China
[b] Xi'an Jiaotong University, Xi'an, China

HIGHLIGHTS

- A 12 month investigation of total suspended particles was conducted in southeastern Tibet Plateau.
- n-Alkanes and polycyclic hydrocarbons were emitted by both anthropogenic and natural emissions.
- Biomass burning in the residential heating season was an important source of PAHs.

ARTICLE INFO

ABSTRACT

Sixty-two suspended particle (TSP) samples were collected from Lulang on the southeastern Tibetan Plateau from July 2008 and July 2009 to investigate the concentrations, seasonal variations, and sources of n-alkanes and polycyclic aromatic hydrocarbons (PAHs). Samples were analyzed using thermal-deposition gas chromatography mass spectrometry. The concentrations of particulate total n-alkanes ranged from 0.10 to 21.83 ng m^{-3}, with an annual mean of 1.25 ng m^{-3}; the PAHs ranged from 0.06 to 2.53, with a mean of 0.59 ngm^{-3}. Up to 70% of PAHs were 5- and 6-ring compounds. The n-alkanes and PAHs both showed higher concentrations in winter and lower concentrations in summer. Analyses of diagnostic ratios indicate that 6.4% to 58.9% (mean 24.9%) of the n-alkanes were from plant waxes. Source characterization studies, i.e. diagnostic ratio and positive factor matrix analysis, suggest that the PAHs were from biomass burning as well as from fossil fuel combustion. Backward trajectory analysis suggests that the biomass mass burning pollutants could be from South Asia and western China via long distance transport. The study contributes to a more comprehensive understanding of the concentrations, seasonal variations, and sources of n-alkanes and PAHs in a remote background area in Tibetan Plateau.

© 2013 Elsevier B.V. All rights reserved.

1. Introduction

The environmental and health impacts of particulate matter (PM) depend on the concentrations, size distributions and chemical composition of the particles. The polycyclic aromatic hydrocarbons (PAHs) and n-alkanes are important anthropogenic components of the secondary organic aerosol. PAHs are mainly emitted into the environment as a result of the incomplete combustion of fossil fuels, but they also originate from natural sources such as biomass (wood, grass) burning (Finlayson-Pitts and Pitts, 2000). As pollutants, PAHs are a health concern because

many of them are known to be carcinogenic, mutagenic, or teratogenic (Albinet et al., 2007). n-Alkanes also are emitted into atmosphere during the incomplete combustion of fossil fuels and biomass, but biogenic sources, especially higher plant waxes, are important for them as well (Simoneit, 2002).

The Tibetan Plateau is sensitive to environmental change, and studies in this area are helpful for better understanding pollution in a remote background area. Reports of PAHs in northwestern China and Tibet are limited (Hu et al., 2012; Li et al., 2012; Liu et al., 2013). The atmospheric PAH research conducted to date has mainly focused on urban areas in southern and eastern China (Bi et al., 2005; Chen et al., 2005; Deng et al., 2006; Duan et al., 2005; Guo et al., 2007; Liu et al., 2001, 2013; Luo et al., 2004, 2006; Okuda et al., 2002; Tan et al., 2006). Our investigation focused on total suspended particles (TSP) from a site on the southeastern side of the Tibetan Plateau. The studies were conducted from

July 2008 and July 2009 at Lulang, and the results demonstrate some impacts of anthropogenic emissions on the southeastern part of the Plateau.

2. Material and methods

2.1. Sampling region and site

A map showing the location of the observation site is provided in Fig. 1. The site is located 6 km north of Lulang Town in Nyingchi (Linzhi) Prefecture, which is on the southeastern part of the Tibetan Plateau, on the northern bank of the Yarlung Zangbo River and downstream from the Nyangchu River. The total area of the prefecture is 10,237 km², the average altitude is 3100 m, and its population in 2007 was ~40,496 (Statistics NBoPaE, 2007). The sampling site is in a valley (longitude 94° 44′E, latitude 29° 46′N), and it is frequently used for environmental investigations in this mountainous region. The sampling site is not directly affected by local anthropogenic emissions. The annual cycle, based on local climate, grouped as follows: autumn (September, October), winter (November, December), spring (March, April, and May) and summer (June, July and August). The circulation at the site is largely under control of two monsoons; this results in westerly winds during winter monsoon and north-westerly winds in summer (Indian Monsoon). As shown in Table 1, the average wind speed, relative humidity (RH), and atmospheric pressure are relatively stable in the four seasons. The highest temperature is in the summer (12.7 °C) and the lowest in winter (−1.6 °C). The pollution episode, starts at late autumn, lasts the whole winter, and ends in spring, also known as local "heating season". The emissions such as local burn wood, grass and yak dung for heating and cooking, constantly impact the local environment. Coal burning is limited locally.

The sampling campaign lasted from July 2008 to July 2009. The sampling instruments were placed on a working platform ~2 m above the

Table 1
Annual and seasonal meteorological data for the southeastern Tibetan Plateau.

Variable	Autumn	Winter	Spring	Summer	Annual
Wind speed (m·s⁻¹)	1.55	1.73	1.83	1.55	1.68
Relative humidity (%)	76.3	66.7	71.2	81.9	73.5
Pressure (hPa)	684.24	681.22	680.80	680.53	681.37
Temperature (°C)	6.9	−1.6	5.4	12.7	5.4

ground. The TSP samples were collected using a KC-120H mid-flow TSP collection system (Laoshan Instruments, Qingdao, China) that operated at a flow of 40 dm³ min⁻¹. The 80 mm diameter quartz filters (Whatman, NJ) used as the collection substrates were heated in an oven at 780 °C for 5 h to combust any organic compounds, and they were stored in aluminum foil before use. Each sample was collected over three days, nominally for 60 h (20 h for collection, and 4 h for instrument maintenance each day). The sample filters were stabilized in a temperature- and humidity-controlled incubator after collection (25 °C, 50% relative humidity) for 24 h. All the filters were weighed using an electronic micro balance (Mettler M3, Switzerland) and stored at 4 °C before analysis. In all, 62 samples were collected during the campaign. A total of 62 samples was collected in four seasons.

2.2. Sample analysis

All of the TSP samples were analyzed by thermal-desorption gas chromatography–mass spectrometry (TD-GC–MS) with the use of an Agilent 7890A/5975C system. Details of the TD-GC–MS procedure have been described elsewhere (Ho et al., 2011). Briefly, each filter was cut into small (~0.5 cm²) pieces, which were then put into a TD glass tube (78 mm long, inner diameter (ID) 4 mm, outer diameter
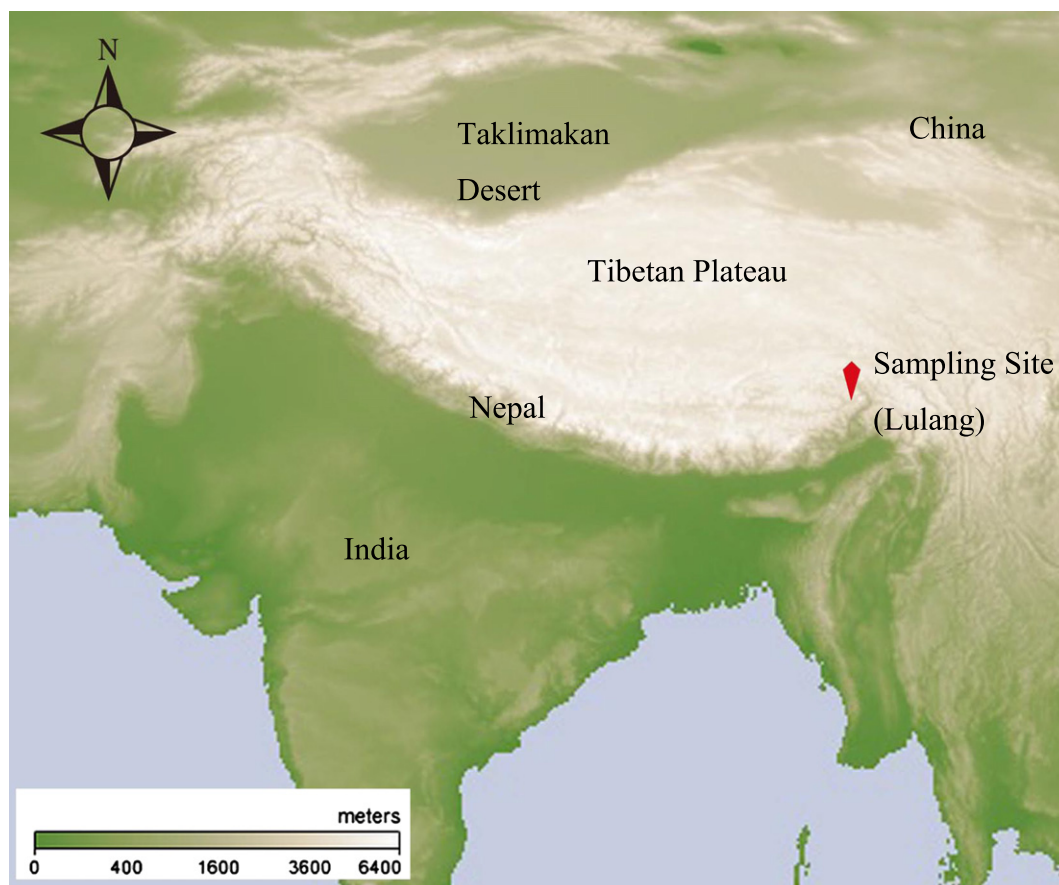

Fig. 1. Map of the sampling site at Lulang, Nychi, southeastern Tibetan Plateau (longitude 94° 44′E, latitude 29° 46′N) from NASA.

(OD) 6.35 mm) in preparation for injection into the instrument. Thermal desorption was used for injection in a splitless mode; the injector temperature was held at 50 °C before analysis and manually raised to 275 °C over 11 min after the septum cap was closed. A capillary column (HP-5 ms: 5% biphenyl/95% dimethylsiloxane; 50 m long × 0.332 mm ID × 0.17 μm film) was used to separate the compounds of interest. The temperature program for the oven was as follows: 30 °C hold for 2 min, then increase from 30 °C to 120 °C at 10 °C min^{-1}, ramp from 120 °C to 325 °C at 8 °C min^{-1}, and finally hold at 325 °C for 20 min; thus the total run time was 52 min (Ho et al., 2011). The helium flow rate for the system was 1.2 cm^3 min^{-1}.

The electron ionization mass spectra (70 eV) were acquired over a mass range (m/z) of 30 to 570 amu, and the selected ion mode was used for quantification. PAHs were identified using both the retention time from the GC chromatograph and comparisons of the MS spectra with standards; the compounds were quantified with the use of an external standard (Ho et al., 2011). The concentrations of 17 PAHs were determined; these were phenanthrene (Phe), anthracene (Ant), fluoranthene (Flu), pyrene (Pyr), benzo[a]anthracene (BaA), chrysene (Chr), benzo[b]fluoranthene (BbF), benzo[k]fluoranthene (BkF) benzo[a]fluoranthene (BaF), benzo[e]pyrene (BeP), benzo[a]pyrene (BaP), perylene (Per), indeno[1,2,3-cd]pyrene (IcdP), dibenzo[a,h]anthracene (DahA), benzo[ghi]perylene (BghiP), coronene (Cor), and dibenzo[a,e]pyrene (DaeP).

2.3. Quality control

Detailed quality assurance/quality control (QA/QC) procedures for analyses have been described elsewhere (Cao et al., 2011; Ho et al., 2006, 2011). In brief, the sampler was checked and cleaned monthly during sampling. Blank filters were used as a background check for the organic compounds. During the GC–MS analysis, one sample was randomly chosen from each group of ten for a replicate analysis. The results indicate that the standard deviation σ for the replicate analyses for each compound was between 1 and 15%, and the uncertainties in the concentrations were between 0.0073 and 0.001 ng m^{-3}.

2.4. Source diagnostics

2.4.1. Sources for n-alkanes

Two diagnostic measures, the carbon maximum number (C_{max}) and carbon preference index (CPI) have been commonly used to evaluate the sources for n-alkanes (Simoneit, 1984, 1999; Simoneit and Mazurek, 1982). C_{max} is a general indicator of the relative contributions of two n-alkane sources. That is, higher values for C_{max} indicate that the n-alkanes primarily originated from terrestrial plants, especially epicuticular waxes while lower C_{max} values are more consistent with n-alkanes from anthropogenic sources.

The CPI (plural CPIs) is defined as the sum of the concentrations of the odd carbon-number n-alkanes divided by the sum of the concentrations of the even carbon number n-alkanes. The n-alkanes that originate from terrestrial vegetation typically exhibit high values for the CPI, that is, a strong odd over even carbon number preference. The CPI values for emissions from motor vehicles and other anthropogenic sources, in contrast, are close to unity. The CPIs for the n-alkanes are often calculated in several ways as follows:

For all n-alkanes measured in this study:

$$CPI_1 = \sum (C_{19} - C_{35}) / \sum (C_{18} - C_{34}) \qquad (1)$$

for the petrogenic n-alkanes

$$CPI_2 = \sum (C_{19} - C_{25}) / \sum (C_{18} - C_{24}) \qquad (2)$$

and for the biogenic n-alkanes

$$CPI_3 = \sum (C_{27} - C_{35}) / \sum (C_{26} - C_{34}). \qquad (3)$$

For each odd-numbered carbon n-alkane (C_n), the mass contributed by plant waxes can be estimated by subtracting from its measured concentration the average of the even-numbered homologues with one greater and one fewer carbon atoms as follows:

$$Wax\ C_n = [C_n] - [C_{n+1} + C_{n-1}] \times 0.5. \qquad (4)$$

Here the quantities in brackets are the n-alkane concentrations in the sample. The percent plant wax contributions to the total mass of the measured n-alkanes can then be calculated as the sum of the wax masses for the odd carbon n-alkanes divided by the total n-alkane mass times 100.

2.4.2. Sources for PAHs

PAHs are released into environment through both pyrogenic and petrogenic processes; these terms relate to the temperature at which the compounds are formed and hence the temperature of alkylation (Simoneit, 2002). More specifically, pyrogenic processes include the combustion of organic matter during industrial activities, residential heating, power generation, waste incineration, and the operation of motor vehicles (Li et al., 2008).

Chemical markers and diagnostic ratios are tools used to assess the sources for organic aerosol particles (Cotham and Bidleman, 1995). Three diagnostic ratios of PAHs, (1) Ant/(Phe + Ant), (2) Flu/(Flu + Pyr), and (3) IcdP/(IcdP + BghiP) were used here to identify likely sources for the PAHs. The ratios reflect the importance of specific sources including the combustion of oil and coal, diesel and automobile emissions. These four ratios are discussed in the context of the results in Section 3.5.

2.4.3. PMF analysis of PAHs

Positive Matrix Factorization (PMF) was used for the source characterization of PAHs. PMF can identify factors of covariant species, with considering measurement uncertainties (Paatero and Tapper, 1994). The details of PMF analysis was described elsewhere (Juntto and Paatero, 1994; Lee et al., 2004; Ma et al., 2010; Moon et al., 2008; Paatero and Tapper, 1994). We used the EPA PMF ver. 3.0, and choose 16 PAHs in 62 days (covered a year). Random seed mode and random starting point were chosen.

3. Results and discussion

3.1. n-Alkanes

A set of 18 n-alkanes (C_{19}–C_{36}) was measured for the study, and a summary of the total and average concentrations of these compounds and the PAHs is presented in Table 2. With a mean of 0.18 ng m^{-3}, C_{31} was the most abundant of the n-alkane homologues; the next most abundant was C_{29} (0.16 ng m^{-3}). Most of the average concentrations of n-alkanes were <0.10 ng m^{-3}. The seasonally-averaged sums of the measured n-alkane concentrations ($\sum$ n-alkanes) ranged from 0.10 to 20.83 ng m^{-3}, with an overall mean for the entire study of 1.25 ng m^{-3}. The seasonal variation of the mass concentrations of the $\sum$ n-alkanes is presented in the form of a pie chart in Fig. 2a; they decreased from spring (29.85%) to winter (25.58%) to autumn (23.24%) to summer (21.26%).

In general, the $\sum$ n-alkane concentrations were relatively stable, but there were several spikes in the concentrations of these compounds (Fig. 2a). The highest $\sum$ n-alkane concentration was 24.53 ng m^{-3}, and that peak occurred on 3 February 2009. In comparison, during the rest of the year, the concentrations of $\sum$ n-alkanes were <5 ng m^{-3}, suggesting that the February spike was caused by a pollution event e.g. forest fire. The average $\sum$ n-alkane concentration was much lower than even the minimum concentrations observed in several other urban areas in China. For comparison, the $\sum$ n-alkanes at Beijing were 163.0 ± 193.5 ng m^{-3} in PM$_{2.5}$ (Huang et al., 2006); at Baoji they

Table 2
Concentration (ng m^{-3}) of n-alkanes and polycyclic aromatic hydrocarbons in total suspended particle samples from the southeastern Tibetan Plateau.

Compound	Abbreviation	Mean	Standard deviation	Range
n-Alkanes				
Nonadecane	C19	0.03	0.03	BDL-0.17
Eicosane	C20	0.02	0.02	BDL-0.08
Heneicosane	C21	0.02	0.02	BDL-0.11
Docosane	C22	0.01	0.02	BDL-0.10
Tricosane	C23	0.02	0.03	BDL-0.19
Tetracosane	C24	0.02	0.03	BDL-0.15
Pentacosane	C25	0.05	0.06	0.01-0.32
Hexacosane	C26	0.04	0.07	BDL-0.51
Heptacosane	C27	0.10	0.23	0.01-1.65
Octacosane	C28	0.08	0.20	BDL-1.57
Nonacosane	C29	0.18	0.50	0.01-3.80
Tricontane	C30	0.08	0.23	0.01-1.79
Hentriacontane	C31	0.18	0.61	0.01-4.73
Dotriacontane	C32	0.05	0.15	BDL-1.12
Tritriacontane	C33	0.16	0.59	0.01-4.64
Tetratriacontane	C34	0.08	0.07	0.01-0.42
Pentatriacontane	C35	0.08	0.13	BDL-0.97
Hexatriacontane	C36	0.05	0.04	BDL-0.18
	SUM	1.25	2.82	0.10-21.83
Polycyclic aromatic hydrocarbons (PAHs)				
Phenanthrene	Phe(3-ring)	0.08	0.07	0.01-0.46
Anthracene	Ant(3-ring)	0.02	0.02	BDL-0.13
Fluoranthene	Flu(4-ring)	0.02	0.01	BDL-0.09
Pyrene	Pyr(4-ring)	0.02	0.02	BDL-0.11
Benzo[a]anthracene	BaA(4-ring)	0.01	0.01	BDL-0.06
Chrysene	Chr(4-ring)	0.02	0.02	BDL-0.09
Benzo[b]fluoranthene	BbF(5-ring)	0.06	0.06	BDL-0.30
Benzo[k]fluoranthene	BkF(5-ring)	0.04	0.04	BDL-0.18
Benzo[a]fluoranthene	BaF(5-ring)	0.01	0.01	BDL-0.05
Benzo[e]pyrene	BeP(5-ring)	0.05	0.05	BDL-0.27
Benzo[a]pyrene	BaP(5-ring)	0.03	0.03	BDL-0.15
Perylene	Per(5-ring)	0.01	0.01	BDL-0.04
Indeno[1,2,3-cd]pyrene	IcdP(6-ring)	0.08	0.08	BDL-0.41
Dibenzo[a,h]anthracene	DahA(6-ring)	0.01	0.01	BDL-0.06
Benzo[ghi]perylene	BghiP(6-ring)	0.06	0.06	BDL-0.30
Coronene	Cor(6-ring)	0.03	0.03	BDL-0.18
Dibenzo[a,e]pyrene	DaeP(6-ring)	0.03	0.04	BDL-0.24
	SUM	0.59	0.52	0.07-2.63

Note: BDL means below detection limits. The PAHs and the number of fused benzene rings are marked in the abbreviation.

were 449 ng m^{-3} in spring and 1733 ng m^{-3} in winter in PM$_{10}$ samples (Xie et al., 2009); at Guangzhou they were 141 to 392 ng m^{-3} in PM$_{10}$ (Bi et al., 2002); at Hong Kong they averaged 23.5 ng m^{-3} in
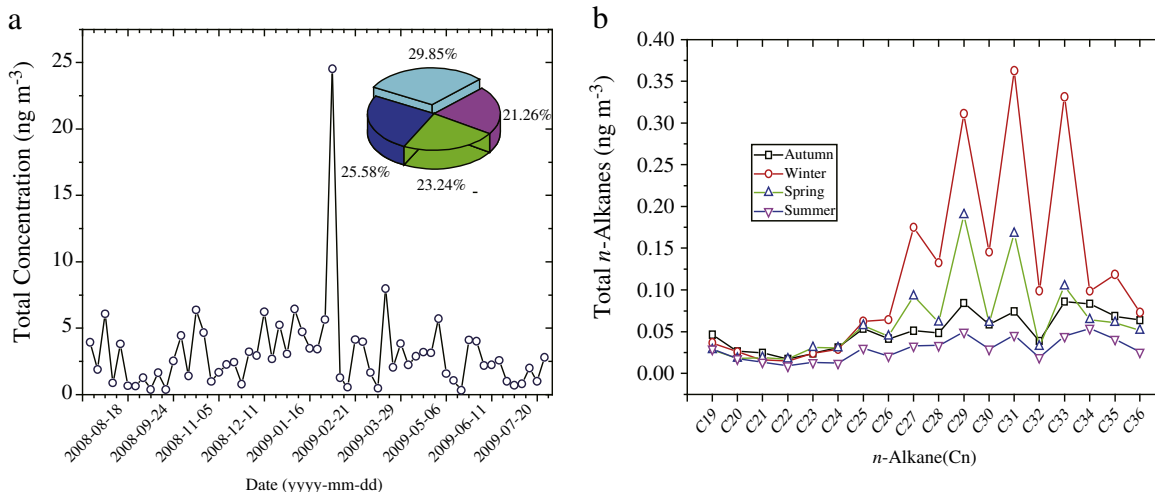
Table 3
Summary of the concentration of n-alkanes and PAHs in this study and other remote background areas in the world.

Location	Conc.(ng m^{-3})	Reference
PAHs		
Lulang, Tibet	0.06–2.53	This study
Bavaria, Norway	2–4	Schönbuchner et al. (2001)
Finland	1–6.3	Rissanen et al. (2006)
North Pacific Ocean/Arctic area	4.38	Ding et al. (2007)
Finokalia, Island of Crete	0.6–1.8	Tsapakis and Stephanou (2007)
Lake Michigan	14	Cotham and Bidleman (1995)
Remote Europe Lake	1.8–3.0	Fernández et al. (2003)
Tyrolean Alps, Europe	0.20	Drooge et al. (2010)
Tenerife	0.06	Drooge et al. (2010)
Central Norway	0.38	Drooge et al. (2010)
n-Alkanes		
Lulang, Tibet	1.25	This study
Hillside and Meteor Crater, US	11.3–41.4	Mazurek et al. (1991)
Finland	7–95	Rissanen et al. (2006)

PM$_{2.5}$ (Zheng et al., 2000); at Algier city, Algeria they were 14.3 to 142 ng m^{-3} from May to September PM$_{10}$ (Yassaa et al., 2001). On the other hand, the observed $\sum n$-alkanes at Lulang were comparable with those reported for some remote areas, such a forest in Finland (7–95 ng m^{-3}) (Rissanen et al., 2006) or Umeå, Sweden (8.2 ng m^{-3} in PM$_{2.5}$, (Wingfors et al., 2011)). The summary of the results from this study and other remote area is listed in Table 3.

3.2. n-Alkane seasonal variations and source characterization

The patterns of the n-alkanes as a function of carbon number showed some similarities among the four seasons, and Fig. 2b shows how the concentration of each n-alkane varied with season. Indeed, the patterns in the relative abundances of the n-alkanes can be explained by considering the variations in their source contributions. The C$_{max}$ values ranged from C$_{29}$ to C$_{33}$ (Fig. 2b), and these high carbon numbers suggest that biological materials, especially epicuticular waxes from higher plant, were stronger sources for these compounds than anthropogenic emissions (Simoneit, 2002). The calculations of the percent plant wax mass contributions indicate that the highest contributions occurred in spring (32.37%), followed by winter (27.88%), summer (18.51%), and autumn (17.09%) (Table 4). In spring, the biogenic activities, such as the changing of leaves, blooming, fungi and pollen spreading, are stronger than in summer, contributing more n-alkanes

Fig. 2. Concentrations of $\sum n$-Alkanes in TSP from the southeastern Tibetan Plateau from July 2008 to July 2009. In the pie chart, cyan, purple, green and blue indicate spring, summer, autumn, and winter, respectively; seasonal variation of $\sum n$-alkanes in the TSP in the southeast of Tibetan Plateau during July 2008–July 2009 (b).

Table 4
Diagnostic indices and ratios of *n*-alkanes and PAHs in the different seasons in southeastern Tibetan Plateau from July 2008–July 2009.

Index or ratio	Autumn		Winter		Spring		Summer		Annual	
	Mean	Range	Mean	Range	Mean	Range	Mean	Range	Mean	Range
CPI_1[a]	1.31	1.05–1.91	1.64	1.05–2.85	1.95	1.13–3.63	1.36	1.11–1.82	1.59	1.05–3.63
CPI_2[b]	1.27	0.78–1.71	1.24	0.56–1.68	1.33	1.09–1.73	1.44	0.94–2.36	1.32	0.56–2.36
CPI_3[c]	1.32	1.01–2.16	1.77	0.98–3.15	2.29	1.10–4.69	1.32	0.98–1.93	1.71	0.98–4.69
% wax[d]	17.09	6.38–34.35	27.88	12.47–48.46	32.37	9.72–58.88	18.51	10.14–34.24	24.78	6.38–58.88
Ant/(Phe + Ant)	0.28	0.21–0.36	0.24	0.18–0.33	0.25	0.16–0.37	0.25	0.18–0.30	0.25	0.16–0.37
Flu/(Flu + Pyr)	0.46	0.38–0.57	0.40	0.36–0.45	0.44	0.37–0.51	0.43	0.34–0.52	0.43	0.34–0.57
IcdP/(IcdP + BghiP)	0.54	0.45–0.58	0.57	0.54–0.60	0.55	0.49–0.60	0.55	0.48–0.60	0.56	0.45–0.60

[a] $CPI_1 = (all~n\text{-alkanes}) = \sum(C_{19} - C_{35}) / \sum(C_{18} - C_{34})$.
[b] CPI_2 (petrogenic *n*-alkanes) $= \sum(C_{19} - C_{25}) / \sum(C_{18} - C_{24})$.
[c] CPI_3 (biogenic *n*-alkanes) $= \sum(C_{27} - C_{35}) / \sum(C_{26} - C_{34})$.
[d] Wax $C_n = [C_n] - [C_{n+1} + C_{n-1}] \times 0.5$.

in TSP summer which is the tourist season in the whole year, with more anthropogenic activities; meanwhile, the Indian monsoon bring more biomass burning pollutants by long distance transport (see Section 3.7). Therefore, contribution of epicuticular wax decreases in summer.

Table 4 also shows the calculated values for CPI_1, CPI_2, and CPI_3 for the four seasons and the entire study: CPI_1 ranged from 1.05 to 3.63 over the course of the study, with a mean value of 1.59; this attests to variable but significant impacts from both biogenic and anthropogenic sources. For the compounds with more than 24 carbons, the odd carbon-number *n*-alkanes showed higher concentrations compared with the two nearest even-number homologs. The high values for CPI_1 suggest a strong contribution of terrestrial plant waxes, but for some samples CPI_1 approached unity, and in those samples the *n*-alkanes were more than likely from pollution emissions.

The ranges for CPI_1 in autumn and summer were similar, 1.05–1.91 and 1.11–1.82, respectively, suggesting that there were similar impacts from petroleum sources in those two seasons (also shown in Fig. 6 for PAHs). Consistent with the high wax mass contribution in spring noted above, the highest CPI_1 also occurred in that season (3.63), and supports the conclusion that the largest impact from biogenic sources occurred during the growing season. In winter CPI_1 showed a range of 1.05–2.85 and mean of 1.64; this is an indication that the *n*-alkane loadings in winter were affected by both petrogenic emissions and biomass burning (Rogge et al., 1993a,b; Schauer et al., 1996). The wintertime mean CPI_1 was higher than those reported for several Chinese cities, such as Nanning (1.2–1.4, average 1.3; (Wang and Kawamura, 2005)), Baoji (1.1–1.5, average 1.3 in winter; (Xie et al., 2009)), Hong Kong (1.3–1.9, average 1.6; (Zheng et al., 2000)), and Beijing (average 1.6; (Huang et al., 2006)). This result is also higher than for a forest in Finland (0.8–2.3, average 1.1; (Rissanen et al., 2006)).

CPI_2 ranged from 0.56 to 2.36 over the course of the study (Table 4), and the fact that all of the seasonal means were greater than unity shows that anthropogenic sources affected the *n*-alkanes throughout the year. The seasonal means for CPI_2 varied from 1.27 to 1.44, implying similar contributions from petrogenic sources throughout the year, and these were most likely associated with the transportation sector. CPI_3 was more variable compared with CPI_2: CPI_3 showed a range of 0.98–4.68, and this variability shows that the influence of biogenic emissions changed considerably from season-to-season. The seasonal means for CPI_3 were the lowest (1.32) in both autumn 2008 and summer 2009; it increased in winter to 1.77, probably as a result of biomass burning and reached its highest value (2.29) in spring. This is another indication that the greatest biogenic influences on the *n*-alkanes occurred in spring.

The highest loadings of the *n*-alkanes occurred during the winter heating season, and this can be explained by the large quantities of *n*-alkanes emitted when biomass is burned for home heating. Thus, the profiles of the aerosol *n*-alkanes were influenced by both anthropogenic and biogenic emissions, but the relative strengths of these sources varied with season. In spring, the major sources for *n*-alkanes were biogenic while in winter impacts from biomass burning were evident. The balance between biogenic and anthropogenic sources shifted toward the latter in summer and autumn, and the relative impacts of those sources, at least as measured by the CPI_3 index were similar in those two seasons.
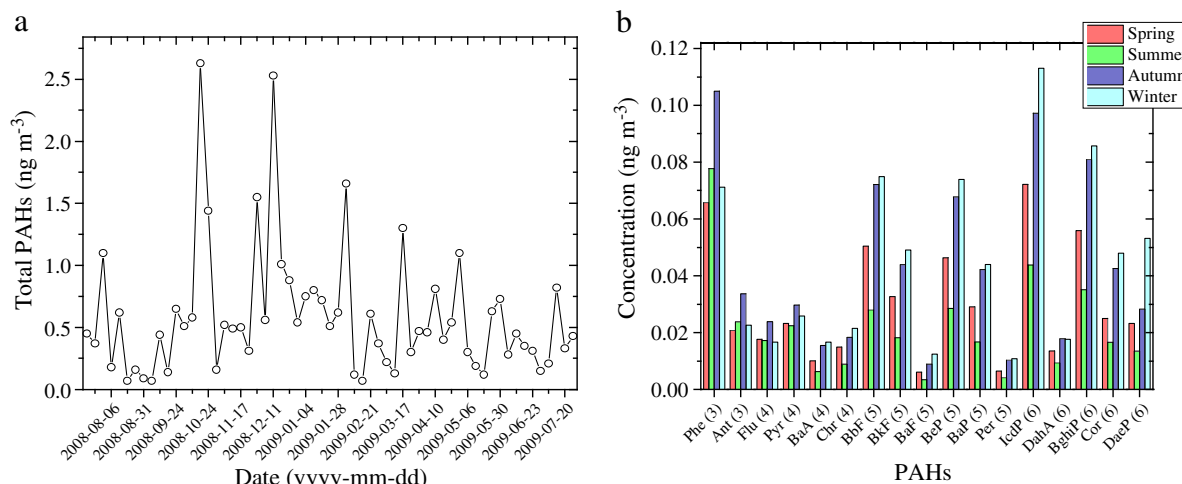

Fig. 3. Annually averaged PAH concentration in TSP from the Lulang site on the southeastern Tibetan Plateau during July 2008 and July 2009 (a); characterization of specific particulate polycyclic aromatic hydrocarbons (PAHs) from the southeastern Tibetan Plateau in four seasons between July 2008 and July 2009 (b).
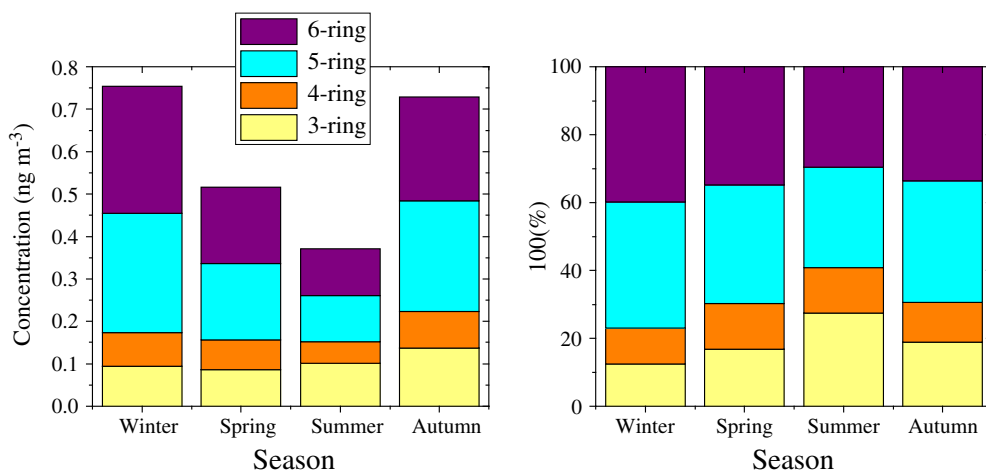
Fig. 4. Observed (left) and normalized (right) seasonal variations of particulate PAHs with different numbers of rings.

3.3. PAH concentrations

The combined sum of the PAH concentrations (total PAHs or $\sum$PAHs) ranged from 0.07 to 2.63 ng m^{-3}, and the overall average $\sum$PAHs was 0.59 ng m^{-3}. A time-series plot of $\sum$PAHs (Fig. 3a) shows that the highest concentration occurred on 18 October 2008 and that in most cases, $\sum$PAHs < 0.5 ng m^{-3}. These typical observed $\sum$PAH values were much lower than what has been reported for urban areas in China. For example, at Lhasa city, $\sum$PAHs in TSP was 10 ± 6.6 ng m^{-3} and 20 ± 15 ngm^{-3} in two different sites in summer (Liu et al., 2013); the mean total $\sum$PAHs was 104 ± 130 ng m^{-3} in particle phase from Beijing during the 29th Olympic Games (Ma et al., 2011), Harbin (100 ± 94 ng m^{-3}) (Tian et al., 2009). The summary of the results of this study and other remote areas are listed in Table 3.

The abundances of 17 PAHs in TSP samples were determined for this study, and the range in concentration for each PAH and its mean value

are shown in Table 2. The most abundant PAHs were Phe (3-ring), BbF (5-ring), BeP (5-ring), IcdP (5-ring) and BghiP (6-ring), with yearly average concentrations of 0.08 ng m^{-3}, 0.06 ng m^{-3}, 0.05 ng m^{-3}, 0.08 ng m^{-3} and 0.06 ng m^{-3}, respectively. The annual percent contributions of the five most abundant compounds relative to $\sum$PAHs were as follows: 13.04% (Phe), 9.43% (BbF), 9.12% (BeP), 13.84% (IcdP) and 10.82% (BghiP). These five PAHs accounted approximately 56.25% of the $\sum$PAH mass loadings. In addition, benzo[a]pyrene (BaP), which is commonly used as a marker for PAHs (Wang et al., 2011), showed a range in concentration from below detection to 0.15 ng m^{-3} and a yearly average concentration of 0.03 ngm^{-3}.

It is worth mentioning that Li et al. (2012) reported high concentrations of PAHs in indoor (tent) air in a study conducted during summer in the southern part of the Tibet Plateau. These authors reported that $\sum$PAH and BaP concentrations in air from inside the tents were 5372.45 and 364.79 ng m^{-3}, respectively, and these high loadings
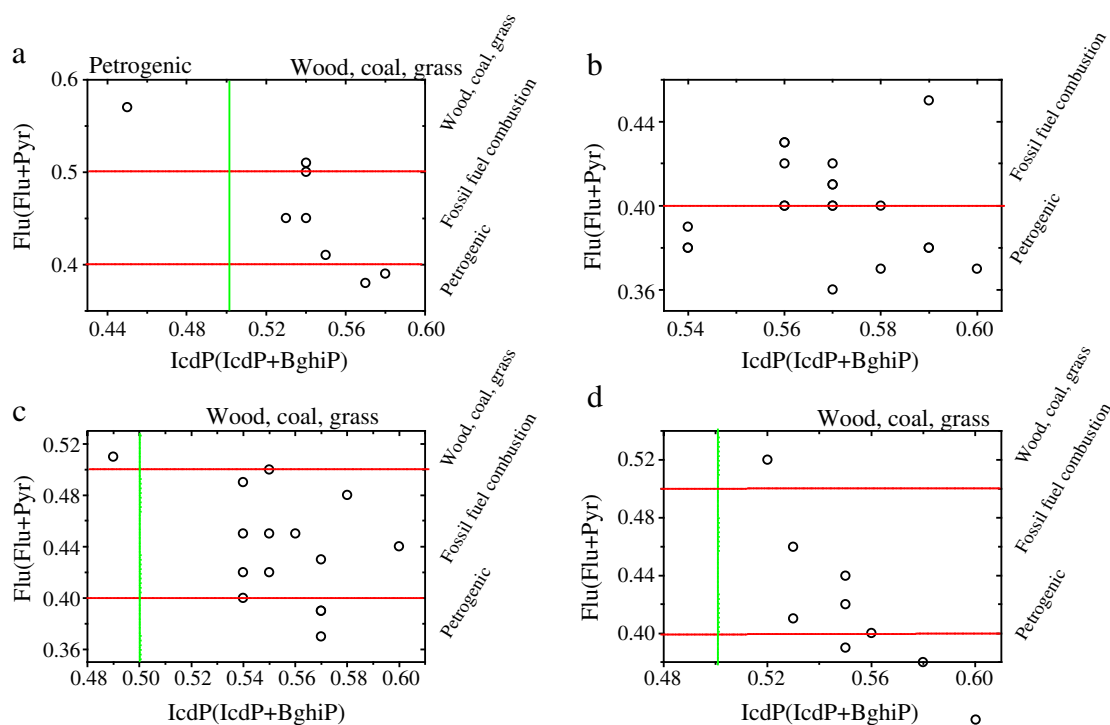

Fig. 5. Diagnostic ratios of Flu/(Flu + Pyr) vs. IcdP/(IcdP + BghiP) in TSP from four seasons: (a) autumn, (b) winter, (c) spring, and (d) summer samples.

were attributed to emissions from residential activates e.g. cooking and heating. These activates thus represent a potentially important regional source for PAHs in ambient air.

3.4. Seasonal variations in PAHs

A more detailed picture of seasonal variations of 17 individual PAHs is shown in Fig. 3b. Most light PAHs (3- and 4-ring compounds) showed similar abundances in the four seasons, the exception was the semi-volatile compound Phe. In contrast, the heavy PAHs (4 or more rings) shared a common pattern; that is, their abundances were low in summer and spring but high in autumn and winter. The total PAH mass concentrations showed a similar seasonal trend, that is, summer (0.37 ng m^{-3}) < spring (0.51 ng m^{-3}) < autumn (0.74 ng m^{-3}) < winter (0.76 ng m^{-3}). The summertime is rain season of local area, resulting in the decreasing of particulate matter by wet deposition.

The distribution of the particulate PAHs as a function of aromatic ring number also changed with season, and the observed and normalized mean mass concentrations of the 3- to 6-ring PAHs are plotted by season in Fig. 4. The normalized plot (right) shows that the concentrations of the 3-ring PAHs were relatively stable, varying from 17% in winter to 25% in summer. The 4-ring PAHs also showed even lower variability, from 5% to 7%. The 5-ring PAHs varied from 30% (summer) to 37% (winter), and the 6-ring from 30% (summer) to 39% (winter). Annually, the 5-ring and 6-ring PAHs were the most abundant PAHs in TSP. The combination of 5- and 6-ring PAHs accounted for ~60–77% of PAHs during the study. All the 5- and 6-ring PAHs showed a seasonal pattern that the mass concentration followed the order that winter > autumn > spring > summer (Fig. 4). Thus, the heavy (5- and 6-ring) PAHs, which are from wood burning, yak dung burning and gasoline and diesel vehicle emissions (Ravindra et al., 2008), showed greater loadings than the lighter (3- and 4-ring) PAHs, which typically are from coal combustion (Chen et al., 2005; Xie et al., 2009). The results
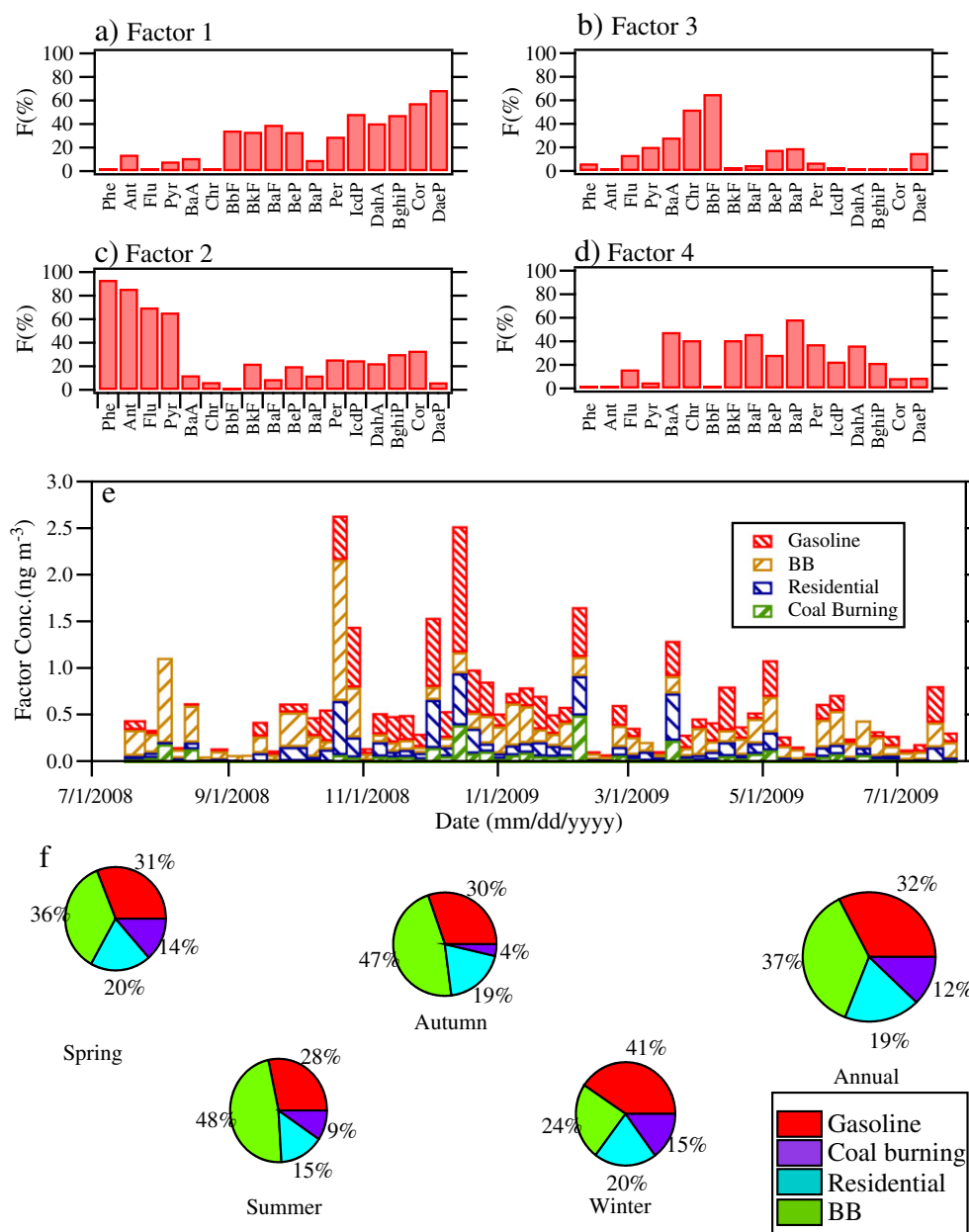

Fig. 6. PAH PMF analysis results: (a), (b), (c), and (d), profile of 4 factors, respectively; (e), time trend of contribution of each factor; (f), pie chart of seasonal and annual contribution of 4 factors. BB stands for biomass burning.

of our study are similar to those reported for Lhasa, the administrative capital of Tibet, that the 5- and 6-ring PAHs were predominant in relative abundance (Liu et al., 2013). See the more detailed results from Section 3.6, PMF analysis.

3.5. PAH source characterization

As shown in Table 4, Ant/(Phe + Ant) ranged from 0.16 to 0.37 over the course of the study, and this supports the contention that most of the PAHs were from pyrogenic sources (Yunker et al., 2002). For a more detail analysis of sources, the diagnostic ratios of Flu/(Flu + Pyr) versus IcdP/(IcdP + BghiP) for the four seasons are plotted in Fig. 5. As shown in Fig. 5a, the IcdP/(IcdP + BghiP) ratios indicate that most of PAHs in autumn were from wood, coal, and grass burning while the Flu/(Flu + Pyr) ratio suggests that PAHs were mainly from fossil fuel combustion and petrogenic sources. The conflicting results suggest the possibility that some PAHs resulted from the long-range transport of pollutants from South Asia (Section 3.7). In winter, the IcdP/(IcdP + BghiP) indicates that most PAHs emission were from combustion and petrogenic emissions (Fig. 5b), the latter probably from local transportation sources and the long-range-transport of pollutants from residential areas in western China (see Section 3.7). Local emissions in the winter were probably from wood, grass, and yak dung which are extensively burned for heat.

The heating season ends with the coming of spring (Fig. 5c); however fossil fuels used for transportation were still important, and a similar pattern appeared in summer (Fig. 5d). Thus, the major sources of PAHs for the entire year were related to the burning of wood, biomass, and yak dung, as well as transportation. Moreover, as noted above, this area of the Tibet Plateau is subject to the transport of pollutants from

India and northwestern China. Therefore, the results of our study demonstrate that the organic aerosol from the southeastern part of the plateau is affected by sources, transport and transformation.

3.6. PMF analysis

4 factors were obtained in PMF analysis for this study. Each profile was compared with the reported ones in the reported previous work. 3 distinct sources and 1 residential were identified. 3 sources are coal burning, biomass burning and gasoline engine exhaust (petrogenic). The identification of factor has to combine with their contributions with seasonal variation. The factor profile, time-concentration trend of factor contributions, seasonal and annual pie charts are shown in Fig. 6.

Factor 1 (Fig. 6a) mostly consists of high molecule weight PAHs, which is similar to gasoline vehicle exhaust (Rogge et al., 1993a,b). Fig. 6e shows that, the contribution of gasoline vehicle exhaust did not show a clear time trend. Fig. 6f showed that, the contribution of petrogenic sources in spring, summer, autumn and winter was 31%, 28%, 30% and 41%, respectively. The annual contribution was stable, ~32%. Factor 2 (Fig. 6b) mainly consists of 3- or 4-ring PAHs. A similar profile was given for biomass burning (Jenkins et al., 1996). The factor concentration of biomass burning showed a strong trend in summer (48%) and weak trend in winter (24%). There are possibly two reasons: in summer, the local PAHs were under influence of India monsoon and brought biomass burning pollutant from the India (see Section 3.7). The annual contribution of biomass burning is 37%, the largest emission source of local PAHs. The profile of factor 3 (Fig. 6c) is similar to that for residential coal combustion (Zheng et al., 2005). Coal burning is a minor source of PAHs, taking up to 12% annually. Factor 4 (Fig. 6d) cannot be identified, compared with the reported profile of PAH emissions.
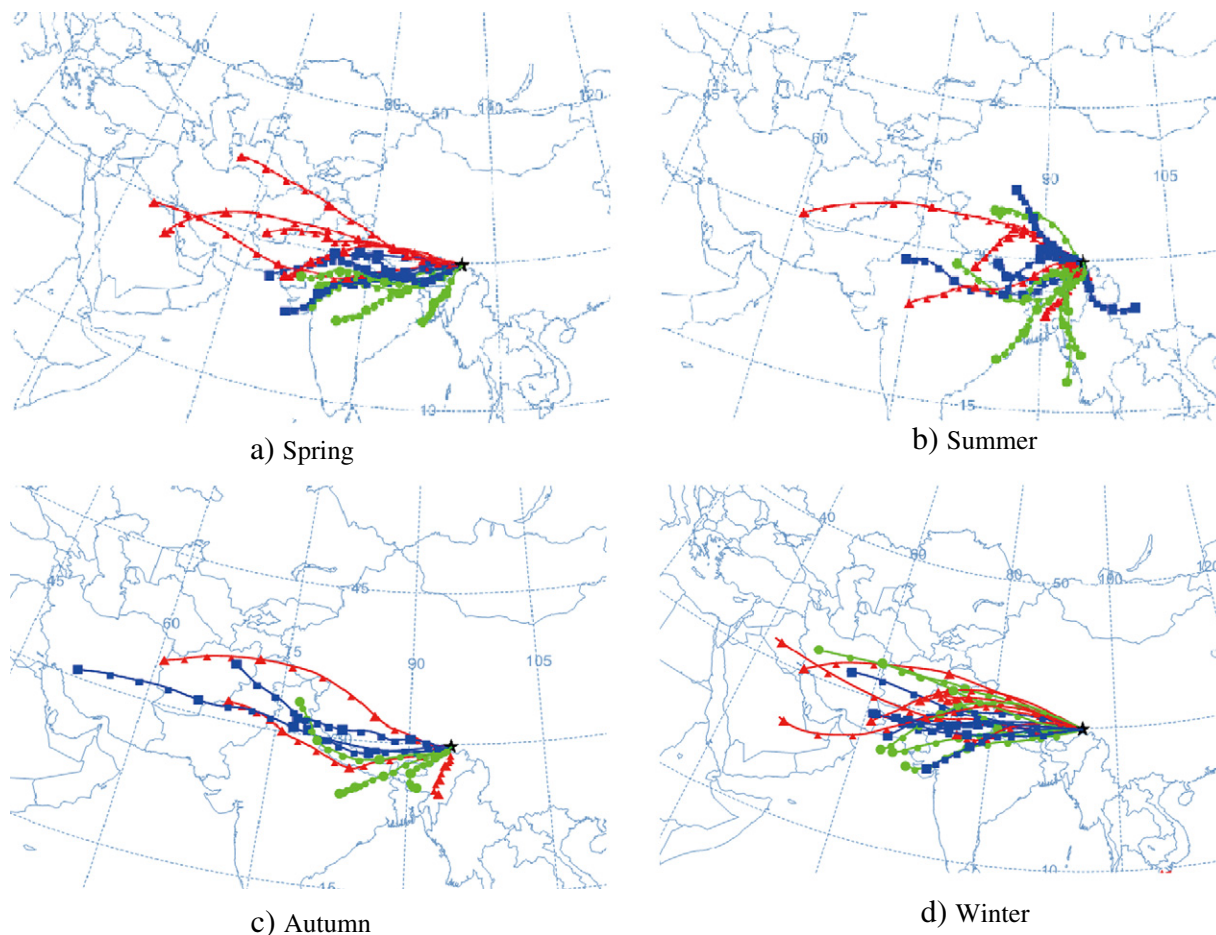

a) Spring

b) Summer

c) Autumn

d) Winter

Fig. 7. Backward trajectory analysis of the sampling site area, starting at UTC 0000 in 72 h, 3000 m altitude in 4 seasons.

Its seasonal variation showed a trend of strong in spring, autumn and winter (~20%) and weak in spring and summer (15%), which is strongly related to the residential heating e.g. yak dung burning for both heating and cooking. Conclusively, the local PAHs were mainly from these 4 factors. Their contributions are in the order of biomass burning > gasoline > residential > coal burning.

3.7. Backward trajectory analysis

Fig. 7 shows the backward trajectory after UTC 0000 for 72 h, with an altitude of 3000 m in each season (http://ready.arl.noaa.gov/HYSPLIT.php). The sampling area is seasonally controlled by west wind (winter) and northwest Indian monsoon (summer). In spring, the air mass comes from two branches: west and southwest (Fig. 7a); in summer, the air mass is mainly from south (Indian Monsoon) (Fig. 7b); in autumn, the air mass is mainly from northwest and south (Fig. 7c); and in winter, the air mass is mostly from the west, passing by the highly populated area (Fig. 7d). Generally, the area of sampling site is influenced by India monsoon and west wind alternatively. Particularly, in summer and autumn (local climate), Indian monsoon brings air mass from south Asia. Biomass burning species could be delivered to China via long distance transport. In winter, west wind from western China populated area delivers pollutant to southeastern Tibetan Plateau. To sum up, the contribution of long distance transport is from India and the populated west area of China.

Zhu et al. (2004) also suggested that high O_3 air masses from eastern/central China, Central/South Asia, and even in Europe contributed significantly to high O_3 in Western China in summer. Air masses from central and eastern China dominated the airflow at northeastern Tibetan Plateau (TP) in summer (Xue et al., 2011). The results from this study suggest that, the air mass influencing southeastern TP is different with northwestern TP.

4. Conclusions and suggestions for further studies

Sixty-two TSP samples were collected at the Lulang observation site on southeastern flank of the Tibet Plateau from July 2008 to July 2009. The study focused on the concentrations, seasonal variations, and sources of particulate n-alkanes and PAHs. Even though the concentrations of the n-alkanes and PAHs in this background area were quite low, the organic aerosol was influenced by both biogenic and anthropogenic emissions. Anthropogenic sources impacted the local environment throughout the year, but the strongest effects were found during winter when large quantities of wood, grass, and dung are burned for residential heating. Both the n-alkanes and the PAHs showed high concentrations in winter because of this, and the concentrations of both groups of compounds were lower in summer. In spring, biogenic influences were evident on the n-alkanes due to the sloughing of epicuticular waxes from higher plants, but the impacts from biological sources were not restricted to the growing season. Indeed, the effects of biological sources on the organic aerosol also were evident in winter, and this was due to the burning of the aforementioned fuels for heating coupled with the fact that comparatively little coal is burned for this purpose.

The information acquired in this study will be useful for understanding how the types of fuels used for heating, transportation, etc. affect the concentrations and types of n-alkanes and PAHs in the atmosphere and the implications of the choices regarding fuel usage for the local environment. This area of the Tibetan Plateau is also potentially subject to emissions caused by biomass burning in India because the large-scale circulation driven by the Indian monsoon favors transport from that direction. Consequently, studies linking the formation of decomposition products for the n-alkanes, such as alkanoic acid, and PAHs (for example, oxygenated-PAHs and nitro-PAHs) with upwind emissions will be useful for investigations into the aging of the parent organic compounds and the effects of long-range transport in the environment.

Appendix A. Supplementary data

Supplementary data associated with this article can be found in the online version, at http://dx.doi.org/10.1016/j.scitotenv.2013.09.033. These data include Google maps of the most important areas described in this article.

References

Albinet A, Leoz-Garziandia E, Budzinski H, Villenave E. Polycyclic aromatic hydrocarbons (PAHs), nitrated PAHs and oxygenated PAHs in ambient air of the Marseilles area (South of France): concentrations and sources. Sci Total Environ 2007;384:280–92.

Bi X, Sheng G, Peng Pa, Zhang Z, Fu J. Extractable organic matter in PM10 from LiWan district of Guangzhou City, PR China. Sci Total Environ 2002;300:213–28.

Bi X, Sheng G, Peng P, Chen Y, Fu J. Size distribution of n-alkanes and polycyclic aromatic hydrocarbons (PAHs) in urban and rural atmospheres of Guangzhou, China. Atmos Environ 2005;39:477–87.

Cao J, Chow JC, Tao J, Lee S, Watson JG, Ho K, et al. Stable carbon isotopes in aerosols from Chinese cities: influence of fossil fuels. Atmos Environ 2011;45:1359–63.

Chen Y, Sheng G, Bi X, Feng Y, Mai B, Fu J. Emission factors for carbonaceous particles and polycyclic aromatic hydrocarbons from residential coal combustion in China. Environ Sci Technol 2005;39:1861–7.

Cotham WE, Bidleman TF. Polycyclic aromatic hydrocarbons and polychlorinated biphenyls in air at an urban and a rural site near Lake Michigan. Environ Sci Technol 1995;29:2782–9.

Deng W, Louie P, Liu W, Bi X, Fu J, Wong M. Atmospheric levels and cytotoxicity of PAHs and heavy metals in TSP and PM2.5 at an electronic waste recycling site in southeast China. Atmos Environ 2006;40:6945–55.

Ding X, Wang X-M, Xie Z-Q, Xiang C-H, Mai B-X, Sun L-G, et al. Atmospheric polycyclic aromatic hydrocarbons observed over the North Pacific Ocean and the Arctic area: spatial distribution and source identification. Atmos Environ 2007;41:2061–72.

Drooge B, Fernández P, Grimalt J, Stuchlík E, Torres García C, Cuevas E. Atmospheric polycyclic aromatic hydrocarbons in remote European and Atlantic sites located above the boundary mixing layer. Environ Sci Pollut Res Int 2010;17:1207–16.

Duan J, Bi X, Tan J, Sheng G, Fu J. The differences of the size distribution of polycyclic aromatic hydrocarbons (PAHs) between urban and rural sites of Guangzhou, China. Atmos Res 2005;78:190–203.

Fernández P, Carrera G, Grimalt JO, Ventura M, Camarero L, Catalan J, et al. Factors governing the atmospheric deposition of polycyclic aromatic hydrocarbons to remote areas. Environ Sci Technol 2003;37:3261–7.

Finlayson-Pitts BJ, Pitts JN. Chemistry of the upper and lower atmosphere: theory, experiments, and applications. Academic Press; 2000.

Guo W, He M, Yang Z, Lin C, Quan X, Wang H. Distribution of polycyclic aromatic hydrocarbons in water, suspended particulate matter and sediment from Daliao River watershed, China. Chemosphere 2007;68:93.

Ho KF, Lee SC, Cao JJ, Li YS, Chow JC, Watson JG, et al. Variability of organic and elemental carbon, water soluble organic carbon, and isotopes in Hong Kong. Atmos Chem Phys 2006;6:4569–76.

Ho SSH, Chow JC, Watson JG, Ting Ng LP, Kwok Y, Ho KF, et al. Precautions for in-injection port thermal desorption-gas chromatography/mass spectrometry (TD-GC/MS) as applied to aerosol filter samples. Atmos Environ 2011;45:1491–6.

Hu J, Liu CQ, Zhang GP, Zhang YL. Seasonal variation and source apportionment of PAHs in TSP in the atmosphere of Guiyang, Southwest China. Atmos Res 2012;118:271–9.

Huang X-F, He L-Y, Hu M, Zhang Y-H. Annual variation of particulate organic compounds in PM2.5 in the urban atmosphere of Beijing. Atmos Environ 2006;40:2449–58.

Jenkins BM, Jones AD, Turn SQ, Williams RB. Emission factors for polycyclic aromatic hydrocarbons from biomass burning. Environ Sci Technol 1996;30:2462–9.

Juntto S, Paatero P. Analysis of daily precipitation data by positive matrix factorization. Environmetrics 1994;5:127–44.

Lee JH, Gigliotti CL, Offenberg JH, Eisenreich SJ, Turpin BJ. Sources of polycyclic aromatic hydrocarbons to the Hudson River Airshed. Atmos Environ 2004;38:5971–81.

Li YT, Li FB, Chen JJ, Yang GY, Wan HF, Zhang TB, et al. The concentrations, distribution and sources of PAHs in agricultural soils and vegetables from Shunde, Guangdong, China. Environ Monit Assess 2008;139:61–76.

Li C, Kang S, Chen P, Zhang Q, Fang GC. Characterizations of particle-bound trace metals and polycyclic aromatic hydrocarbons (PAHs) within Tibetan tents of south Tibetan Plateau, China. Environ Sci Pollut Res Int 2012;19:1–9.

Liu Y, Zhu L, Shen X. Polycyclic aromatic hydrocarbons (PAHs) in indoor and outdoor air of Hangzhou, China. Environ Sci Technol 2001;35:840–4.

Liu J, Li J, Lin T, Liu D, Xu Y, Chaemfa C, et al. Diurnal and nocturnal variations of PAHs in the Lhasa atmosphere, Tibetan Plateau: implication for local sources and the impact of atmospheric degradation processing. Atmos Res 2013;124:34–43.

Luo X, Mai B, Yang Q, Fu J, Sheng G, Wang Z. Polycyclic aromatic hydrocarbons (PAHs) and organochlorine pesticides in water columns from the Pearl River and the Macao harbor in the Pearl River Delta in South China. Mar Pollut Bull 2004;48:1102–15.

Luo XJ, Chen SJ, Mai BX, Yang QS, Sheng GY, Fu JM. Polycyclic aromatic hydrocarbons in suspended particulate matter and sediments from the Pearl River Estuary and adjacent coastal areas, China. Environ Pollut 2006;139:9–20.

Ma W-L, Li Y-F, Qi H, Sun D-Z, Liu L-Y, Wang D-G. Seasonal variations of sources of polycyclic aromatic hydrocarbons (PAHs) to a northeastern urban city, China. Chemosphere 2010;79:441–7.

Ma W-L, Sun D-Z, Shen W-G, Yang M, Qi H, Liu L-Y, et al. Atmospheric concentrations, sources and gas–particle partitioning of PAHs in Beijing after the 29th Olympic Games. Environ Pollut 2011;159:1794–801.

Mazurek MA, Cass GR, Simoneit BRT. Biological input to visibility-reducing aerosol particles in the remote arid southwestern United States. Environ Sci Technol 1991;25: 684–94.

Moon K, Han J, Ghim Y, Kim Y. Source apportionment of fine carbonaceous particles by positive matrix factorization at Gosan background site in East Asia. Environ Int 2008;34:654–64.

Okuda T, Kumata H, Naraoka H, Takada H. Origin of atmospheric polycyclic aromatic hydrocarbons (PAHs) in Chinese cities solved by compound-specific stable carbon isotopic analyses. Org Geochem 2002;33:1737–45.

Paatero P, Tapper U. Positive matrix factorization: a non-negative factor model with optimal utilization of error estimates of data values. Environmetrics 1994;5:111–26.

Ravindra K, Sokhi R, Van Grieken R. Atmospheric polycyclic aromatic hydrocarbons: source attribution, emission factors and regulation. Atmos Environ 2008;42:2895–921.

Rissanen T, Hyötyläinen T, Kallio M, Kronholm J, Kulmala M, Riekkola ML. Characterization of organic compounds in aerosol particles from a coniferous forest by GC–MS. Chemosphere 2006;64:1185–95.

Rogge WF, Hildemann LM, Mazurek MA, Cass GR, Simoneit BRT. Sources of fine organic aerosol. 4. Particulate abrasion products from leaf surfaces of urban plants. Environ Sci Technol 1993a;27:2700–11.

Rogge WF, Hildemann LM, Mazurek MA, Cass GR, Simoneit BRT. Sources of fine organic aerosol. 2. Noncatalyst and catalyst-equipped automobiles and heavy-duty diesel trucks. Environ Sci Technol 1993b;27:636–51.

Schauer JJ, Rogge WF, Hildemann LM, Mazurek MA, Cass GR, Simoneit BRT. Source apportionment of airborne particulate matter using organic compounds as tracers. Atmos Environ 1996;30:3837–55.

Schönbuchner H, Guggenberger G, Peters K, Bergmann H, Zech W. Particle-size distribution of PAH in the air of a remote Norway spruce forest in northern Bavaria. Water Air Soil Pollut 2001;128:355–67.

Simoneit BRT. Organic matter of the troposphere—III. Characterization and sources of petroleum and pyrogenic residues in aerosols over the western United States. Atmos Environ (1967) 1984;18:51–67.

Simoneit BR. A review of biomarker compounds as source indicators and tracers for air pollution. Environ Sci Pollut Res Int 1999;6:159–69.

Simoneit BRT. Biomass burning — a review of organic tracers for smoke from incomplete combustion. Appl Geochem 2002;17:129–62.

Simoneit BRT, Mazurek MA. Organic matter of the troposphere—II. Natural background of biogenic lipid matter in aerosols over the rural western United States. Atmos Environ (1967) 1982;16:2139–59.

Statistics NBoPaE. China population and employment statistics yearbook. China Statistics Press; 2007.

Tan JH, Bi XH, Duan JC, Rahn KA, Sheng GY, Fu JM. Seasonal variation of particulate polycyclic aromatic hydrocarbons associated with PM_{10} in Guangzhou, China. Atmos Res 2006;80:250–62.

Tian F, Chen J, Qiao X, Wang Z, Yang P, Wang D, et al. Sources and seasonal variation of atmospheric polycyclic aromatic hydrocarbons in Dalian, China: factor analysis with non-negative constraints combined with local source fingerprints. Atmos Environ 2009;43:2747–53.

Tsapakis M, Stephanou EG. Diurnal cycle of PAHs, nitro-PAHs, and oxy-PAHs in a high oxidation capacity marine background atmosphere. Environ Sci Technol 2007;41:8011–7.

Wang G, Kawamura K. Molecular characteristics of urban organic aerosols from Nanjing: a case study of a mega-city in China. Environ Sci Technol 2005;39:7430–8.

Wang W, Simonich SLM, Wang W, Giri B, Zhao J, Xue M, et al. Atmospheric polycyclic aromatic hydrocarbon concentrations and gas/particle partitioning at background, rural village and urban sites in the North China Plain. Atmos Res 2011;99:197–206.

Wingfors H, Hägglund L, Magnusson R. Characterization of the size-distribution of aerosols and particle-bound content of oxygenated PAHs, PAHs, and n-alkanes in urban environments in Afghanistan. Atmos Environ 2011;45:4360–9.

Xie M, Wang G, Hu S, Han Q, Xu Y, Gao Z. Aliphatic alkanes and polycyclic aromatic hydrocarbons in atmospheric PM10 aerosols from Baoji, China: implications for coal burning. Atmos Res 2009;93:840–8.

Xue L, Wang T, Zhang J, Zhang X, Poon C, Ding A, et al. Source of surface ozone and reactive nitrogen speciation at Mount Waliguan in western China: new insights from the 2006 summer study. J Geophys Res D (1984–2012) 2011;116:D07306.

Yassaa N, Youcef Meklati B, Cecinato A, Marino F. Particulate n-alkanes, n-alkanoic acids and polycyclic aromatic hydrocarbons in the atmosphere of Algiers City Area. Atmos Environ 2001;35:1843–51.

Yunker MB, Macdonald RW, Vingarzan R, Mitchell RH, Goyette D, Sylvestre S. PAHs in the Fraser River basin: a critical appraisal of PAH ratios as indicators of PAH source and composition. Org Geochem 2002;33:489–515.

Zheng M, Fang M, Wang F, To KL. Characterization of the solvent extractable organic compounds in PM2.5 aerosols in Hong Kong. Atmos Environ 2000;34:2691–702.

Zheng M, Salmon LG, Schauer JJ, Zeng L, Kiang CS, Zhang Y, et al. Seasonal trends in PM2.5 source contributions in Beijing, China. Atmos Environ 2005;39:3967–76.

Zhu B, Akimoto H, Wang Z, Sudo K, Tang J, Uno I. Why does surface ozone peak in summertime at Waliguan? Geophys Res Lett 2004;31:L17104.